

# Bio-inspired Collision Detector with Enhanced Selectivity for Ground Robotic Vision System

Qinbing Fu  
10230460@students.lincoln.ac.uk

Shigang Yue  
syue@lincoln.ac.uk

Cheng Hu  
chu@lincoln.ac.uk

Computational Intelligence Laboratory  
Department of Computer Science  
University of Lincoln  
Lincoln, UK

---

## Abstract

There are many ways of building collision-detecting systems. In this paper, we propose a novel collision selective visual neural network inspired by LGMD2 neurons in the juvenile locusts. Such collision-sensitive neuron matures early in the first-aged or even hatching locusts, and is only selective to detect looming dark objects against bright background in depth, represents swooping predators, a situation which is similar to ground robots or vehicles. However, little has been done on modeling LGMD2, let alone its potential applications in robotics and other vision-based areas.

Compared to other collision detectors, our major contributions are first, enhancing the collision selectivity in a bio-inspired way, via constructing a computing efficient visual sensor, and realizing the revealed specific characteristics of LGMD2. Second, we applied the neural network to help near range path navigation of an autonomous ground miniature robot in an arena. We also examined its neural properties through systematic experiments challenged against image streams from a visual sensor of the micro-robot.

## 1 Introduction

The ability to quickly and robustly detect collisions is vital for both animals and robots to initiate proper behaviors, navigate in dynamic environments, and interact with humans. Autonomous robots have applied several kinds of sensors for object detection, such as vision, ultrasound, infra-red, laser, and mini-radar [1, 2, 3, 4]. However, it is still very difficult for a robot to perform well for collision-detecting without human intervention [5, 6]. Visual sensors have evolved as crucial components for the survival of robots exploiting plentiful image cues in the real physical world. Nevertheless, artificial robot vision systems have not yet been able to quickly and cheaply extract wealthy visual information [7, 8, 9].

Nature has provided abundant source of inspirations for artificial visual system. The ability of extracting useful motion cues in real-time should be indispensable for a practical visual system. The images of approaching stimuli always signify danger to an animal. As the result of hundreds-millions-years evolution, the insects, such as the locusts are so brilliant to very

quickly react to emergent danger even in very complex environments. Several decades have witnessed much progress in understanding of cellular mechanisms underlie motion detection circuit [6, 7, 10, 12, 18, 32, 33]. In insects, it is intriguing that many different specialized visual nervous systems incorporate to extract and fuse motion information from dynamic scenes. In the third visual neuropile stack, the lobula region, there are several Lobula Giant Movement Detectors (LGMDs); however, only two among them, the LGMD1 and LGMD2, have been identified so far [22, 25, 26, 29, 31]. Both of them selectively respond to looming objects in depth rigorously with high firing rates. Although LGMD2 shares most neural properties with LGMD1, they have been demonstrated the different collision selectivity [29]. Compared to LGMD1, LGMD2 matures very early in juvenile locusts which mainly live on the ground whereas already represent evasive responses to predators from the sky [31]. Like LGMD1, LGMD2 contributes intrinsically as a piece in the complex vision system.

In last decade, some LGMD1-based neural networks have been successfully utilized in vehicles and robotics helping imminent collision-detecting for paths exploring [9, 28, 30, 34, 35, 36, 37, 38, 39, 40]. Nevertheless, two main defects exist in LGMD1 modeling works: first, the approaching and receding stimulus are not properly distinguished in depth; second, the translating stimulus regularly leads to collision mis-detection. With regard to the LGMD2 research [29], the revealed neural characteristics make it ideal to handle those defects for ground mobile robots and other vision-based platforms. Moreover, since little modeling works have been done on LGMD2 [13], we are prospective to fill this gap via systematically investigation and experiments. Compared to some state-of-the-art collision detectors, such bio-inspired computational models can cope with unpredictable environments without using specific object recognition algorithms.

Some relevant works are presented in Section 2. The neural network description with detailed formulations and parameters setting are illustrated in Section 3. Followed are the robotic experiments. Finally, we give a conclusion.

## 2 Related Work

**Revealed Neural Properties:** An important and unique feature of the LGMD2 neuron is its looming sense is only for light-to-dark luminance change. It is able to detect dark looming objects embedded in the bright background selectively whilst not responding to light objects against the dark background [29]. In comparison with LGMD1, LGMD2 has a firing preference which is for approaching versus recession of dark targets [29]. This trait could be mapped to solve the former mentioned defect. In addition, when stimulated by translating stimulus, both LGMDs neurons were demonstrated to be activated for a short while then inhibited very soon, even early before the end of movement [25, 29]. Nevertheless, LGMD1 computational models likely signal high firing rates resembling the situation of an object approaching, which is not suitable for a practical collision detector.

**ON and OFF Visual Pathways:** Some smart methods were proposed to account for the former defect, *e.g.* statistically monitoring the membrane potential change gradient to discriminate approach from recession [17]. However, it does not reflect the internal physical mechanism in motion detection circuitry. Instead, we propose a biophysical structure to achieve the specific collision selectivity of LGMD2 via investigating ON and OFF visual pathways [7, 8, 10, 33]. As early in 1970s, LGMDs were put forth to be fed by a homogeneous population of afferent ON and OFF polarity cells [23]. And very recently, a case study of LGMD1 exploiting a similar mechanism was modeled and applied in robotic appli-

cation [5]. As a matter of fact, such a circuit has attracted biologist much interest, whereby its foundation remains elusive. It has been demonstrated to play an irreplaceable role in the internal structure of insects underlie motion detection routes, and reveal the fundamental principle of splitting visual signals downstream into parallel channels encoding brightness increments, decrements in ON, OFF pathways respectively [7, 8, 10, 12, 13].

**Signals Competition:** The signal processing within LGMDs neurons depicts a critical race between excitatory and inhibitory flows, which shapes the looming selectivity of such collision-sensitive neurons [15, 16, 25, 29]. Concretely, the brightness increments activate ON cells to elicit onset events, implying the excitation is time-advanced relative to the inhibition; on the contrary, the excitation is assumed to be time-delayed relative to the inhibition, when OFF cells generate offset responses by luminance decrements [5, 16]. Two kinds of inhibitions coexist in the circuitry to compete with excitations: the activation of lateral inhibition is able to cut down the excitation early during the object growing up in the retina; whereas the activation of feed forward inhibition (FFI) contributes tremendously at curtailing the excitation when the object exceeding an angular size [15, 29]. It has been argued the multiplicative computation playing a crucial role in neural sensory processing systems [14, 15], *e.g.* a dominant model for decades is the Elementary Movement Detectors [6]. Such multiplicative operations have been clarified in biological experiments, while its biophysical mechanisms are still unknown. With respect to the relevant experimental and theoretical results [5, 15], in this network, we were consistent with a multiplication being implemented by a subtraction of two logarithmic terms of excitatory and inhibitory streams followed by an exponentiation via activating the firing rate.

### 3 Model Description

In this section, we present the network description with formulations and parameter setting. The core of this framework is the architecture of biased ON and OFF dual-channel, each of which comprises a multiple layers (Fig. 1). The visual input retrieved by each photoreceptor is split into two separated pathways depending on brightness change: the increments flow into ON channels whilst the decrements into OFF channels. We put forth the bias in all ON channels rigorously suppressing them to achieve the particular collision selectivity of LGMD2. In comparison with other vision-based collision-detectors, it is worth emphasizing here the proposed network detects potential collision via reacting to expansion of the object edges, rather than the strategy of recognizing the target or analyzing the scene.

#### 3.1 Network Architecture and Algorithms

**Photoreceptors:** The first layer consists of photoreceptors arranged in a 2-D matrix form. The number of them corresponds to the resolution of receptive field. Each photoreceptor retrieves the luminance change of gray-scale between every two continuous frames:

$$P_{x,y}(t) = (L_{x,y}(t) - L_{x,y}(t-1)) + \sum_i a_i \cdot L_{x,y}(t-i) \quad (1)$$

where  $P_{x,y}(t)$  is the change of luminance corresponds each pixel at frame  $t$ , subscripts  $x$  and  $y$  are the 2-D coordinates.  $L(t)$  and  $L(t-1)$  are the original brightness of two successive frames with  $t$  denoting the current frame and so on. The persistence of luminance change

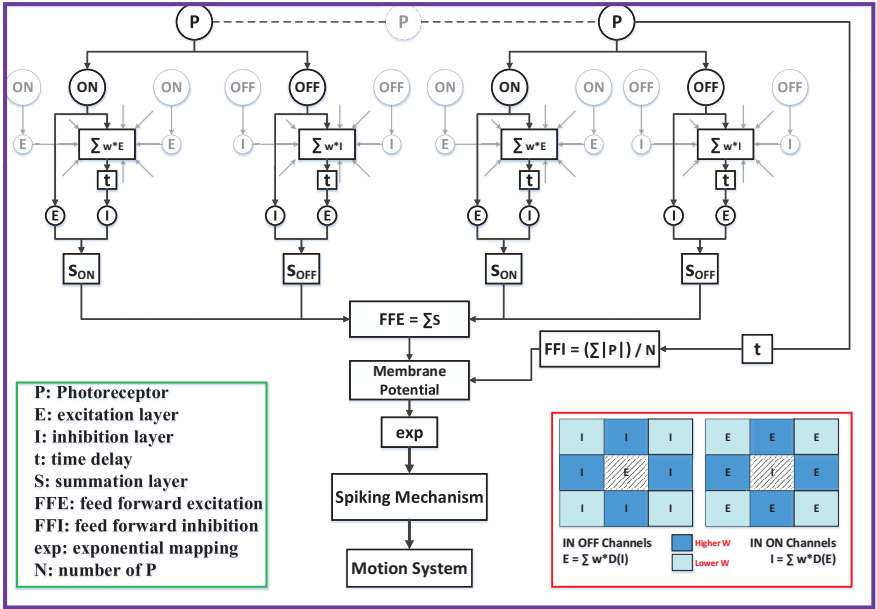


Figure 1: The schematic overview of LGMD2 vision system: Model notations are illustrated in green-box. The convolution illustrations are in red-box. Only two photoreceptors are shown, each of which connects with an ON and OFF cell respectively. ON/OFF units have adjacent gray-cells indicating the center signal is convoluted by the periphery ones (gray), which corresponds to the convolving in red-box. To compute the membrane potential, the FFE pathway integrate all S cells through ON/OFF channels, whereas the FFI pathway retrieves the mean luminance change from all P. More details are presented in Section 3.

could last for a while:  $i$  indicates the number of frames constitute the luminance duration; the coefficient  $a_i$  is defined by  $a_i = (1 + e^{u \cdot i})^{-1}$  and  $u \in (-\infty, +\infty)$ .

**ON and OFF Cells:** There are sufficient densities with an identical quantity as photoreceptors of either ON or OFF afferent cells, arranged to cover the intact retina, respectively eliciting onset and offset events depending on brightness change in each local pixel. As shown in Fig. 1, each photoreceptor corresponds to a pair-wise polarity units. ON cells are activated by the brightness increments, whilst OFF cells by the decrements:

$$P_{x,y}^{ON}(t) = (P_{x,y}(t) + |P_{x,y}(t)|)/2, \quad P_{x,y}^{OFF}(t) = |(P_{x,y}(t) - |P_{x,y}(t)|)|/2 \quad (2)$$

where  $P^{ON}$  denotes the ON cell value and similarity for the OFF cell value  $P^{OFF}$ .

**Multi-layers in ON and OFF Pathways:** With respect to the ON and OFF biophysical mechanism, the visual signals are separated into parallel pathways. First, in ON channels, the output from ON cells forms the input to two individual flows in next Inhibition (I) and Excitation (E) layers (Fig. 1). ON cells elicit onset responses, so that the excitatory flow goes directly to E-Layer and the counterpart cell in the following Summation (S) layer; while the inhibitory flow passes to I-Layer after being convoluted by surrounded delayed excitations:

$$E_{x,y}^{ON}(t) = P_{x,y}^{ON}(t), \quad I_{x,y}^{ON}(t) = \sum_{i=-r}^r \sum_{j=-r}^r E_{x+i,y+j}^{ON}(t-1) \cdot W(i,j), (i \neq j, if i = 0) \quad (3)$$

where  $W$  indicates the local weight matrix as shown in Fig. 1, and  $r$  denotes the kernel radius. It is also clear to notice from Eq. 3, the delayed information are only allowed to spread out to their neighboring cells rather than to their direct counterparts. Similarity for the signal interactions in OFF channels. While comparing to the delayed information in ON pathway, the excitatory flows herein are time delayed relative to the inhibitory flows:

$$I_{x,y}^{OFF}(t) = P_{x,y}^{OFF}(t), \quad E_{x,y}^{OFF}(t) = \sum_{i=-r}^r \sum_{j=-r}^r I_{x+i,y+j}^{OFF}(t-1) \cdot W(i,j), (i \neq j, if i = 0) \quad (4)$$

Followed by are the local summations in S-Layer of polarity channels. The pre-synaptic excitatory and inhibitory flows depict a linear summation:

$$S_{x,y}^{ON}(t) = W_E \cdot E_{x,y}^{ON}(t) - I_{x,y}^{ON}(t), \quad S_{x,y}^{OFF}(t) = E_{x,y}^{OFF}(t) - W_I \cdot I_{x,y}^{OFF}(t) \quad (5)$$

where  $W_E$  and  $W_I$  are two crucial local bias in the LGMD2 modeling work, which could be used to optionally suppress the direct excitatory and inhibitory flows in different pathways. To realize the specific collision selectivity of LGMD2 neurons, we preferred a smaller bias in ON channels rigorously inhibiting the direct excitations. Appropriately adjusting either bias has potential to form an un-biased or even inverse-biased mechanism of the ON and OFF dual-channel.

**Exponential Membrane Potential:** After local summations, as illustrated in Fig. 1, the membrane potential in LGMD2 cell is calculated by two flows. First is the feed forward excitation (FFE) linearly pooling all local cells in S-Layer:

$$FFE(t) = \sum_{x=1}^{row} \sum_{y=1}^{col} S_{x,y}(t) \quad (6)$$

where  $S_{x,y}$  represents all S cells in the dual-channel. *row* and *col* are the rows and columns of S-Layer. Another flow is the feed forward inhibition (FFI) computed via taking the average luminance change of last time step:

$$FFI(t) = \sum_{x=1}^{row} \sum_{y=1}^{col} |P_{x,y}(t-1)| \cdot N^{-1} \quad (7)$$

where  $N = row \cdot col$ . The two feed forward flows depict a logarithmic combination to form the membrane potential which is later exponentially mapped as the model output to invoke the spikes:

$$MP(t) = \log(FFE(t)) - \log(FFI(t) \cdot Coe_{ffi}), \quad EMP(t) = \exp(MP(t)) \quad (8)$$

where  $Coe_{ffi}$  denotes a coefficient adjusting the FFI contribution. In the spiking mechanism, different number of spikes could be elicited in an identical discrete time interval, depending on the exponential distribution of membrane potential:

$$S_t^{spike} = \begin{cases} 0, & \text{if } EMP(t) < T_{sp} \\ 1, & \text{if } T_{sp} \leq EMP(t) < \theta_1 \cdot T_{sp} \\ 2, & \text{if } \theta_1 \cdot T_{sp} \leq EMP(t) < \theta_2 \cdot T_{sp} \\ 4, & \text{else} \end{cases} \quad (9)$$

Parameters: Name, Value					
Name	Value	Name	Value	Name	Value
$col, row$	adaptable	$T_{sp}$	200 ~ 400	$\theta_1$	2.5
$N_{ts}$	4	$W$	0 ~ 0.25	$\theta_2$	5
$N_{sp}$	4 ~ 8	$W_E$	0.1 ~ 0.5	$Coeff_i$	1 ~ 10
$N$	$col \cdot row$	$W_I$	0.3 ~ 1.0	$r$	1

Table 1: The Parameter setting of LGMD2 Vision System

where  $T_{sp}$  denotes the potential threshold level to fire the neuron.  $\theta_1$  and  $\theta_2$  are two constants to partition the potential over threshold into sections. One could allocate higher grades in order to produce more spikes each time. We defined that  $N_{sp}$  numbers of continuous spikes invoked in  $N_{ts}$  successive frames indicates the collision recognition. Due to such a spiking mechanism, the neuron could be activated even in a one-frame step. Finally, the spikes are conveyed to the motion system leading to collision avoidance behaviors (Fig. 1).

### 3.2 Network Parameter Setting

All the free parameters of the proposed LGMD2 visual neural network are based on both empirical and experimental experiences to balance computing and optimize model implementation. No parameter training and learning methods are currently included. The weights of convolution matrix  $W$  in four nearest neighbor positions are higher than those in the diagonal pixels: 0 for the center pixel, 0.25 for the four nearest and 0.125 for the four diagonal ones, pertaining to kernel radius setting at 1. Table 1 lists the major parameters setting-up. The adaptable ones regard to the physical properties of input visual stimulus.

## 4 Experiments and Results

In this section, we move on representing the systematical robotic experiments in real time, along with results and analysis. The main objective is to verify the feasibility and robustness of LGMD2 vision system in robotic applications. An autonomous miniature robot was applied in arena tests, and other sorts of comparative investigations.

### 4.1 Hardware Setting

Both LGMDs vision systems were respectively set up in the ground mobile robot, named 'Colias' (Fig. 2). It is an open-hardware modular micro robot which is developed to be used in swarm robotic applications [8, 12]. Basically the robot platform consists of two main parts. One is the **motion actuator** with diameter of 4cm, which is deployed on the bottom of robot to provide power and motion controls. Two micro DC motors and two diameter 2.2cm wheels are employed to actuate Colias [12]. Another one is the extension **vision module** placed on the top of Colias [12]. A miniature camera is the 'eye' of robot, which is essential in the vision-based control. Such a low-cost camera is able to operate up to 30 frames per second (fps). The angle of view could reach approximately 70 degrees. All these features make the camera suitable for using in micro-robots. We chose a resolution of  $72 \cdot 99$  pixels at 30 fps with the output format of 8-bit YUV422. Its 192 Kbyte internal SRAM supports

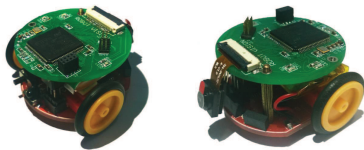


Figure 2: The prototype of Colias: Upper board – vision module, Bottom – motion actuator.

MD – Miss Detection, CD – Correct Detection Success Rate – $SR = [CD/(MD + CD)]\%$			
$T_{sp}$	MD	CD	SR
320	7	58	89.2%
300	3	61	95.3%
280	6	60	90.9%
260	10	55	84.6%

Table 2: Success rate of arena tests under four candidate firing thresholds ( $T_{sp}$ ).

the image buffering and computing. There is a digital camera interface (DCMI) which is an embedded interface for transmitting of the captured images. With the help of a full-duplex serial port, Colias can very quickly send image samples and model data to the hosts.

## 4.2 Arena Tests

We tested the basic collision recognition ability of LGMD2 neural network in an arena with 10 ~ 20 obstacles<sup>1</sup>. The arena was built with inside size of 105cm · 105cm in area. The internal walls and the body of obstacles were drawn with dark patterns. There are also particular patterns on top of the robot and obstacles for the purpose of running a practical multi-robots localization system, rigorously getting the overtime trajectories [□] (Fig. 3). A portable camera was fixed to form a top-down view to capture and record the performances of Colias in arena. The time window was fixed in approximately 60 seconds for each round. Colias autonomously ran in arena and circumvented potential collisions via turning behaviors. We could manually assign avoidance behaviors for Colias, or shut down all of them, depending on experimental requirements. In arena tests, we gave half-half opportunities for Colias to turn a large angle to either direction. The proposed collision detector performed quickly and robustly in the vision-based miniature robot for near range path exploring (Fig. 3); moreover, the model processing with decision making timing of each turn is within 30 milliseconds, which is very suitable to be implemented in real time, shedding light on helping navigation of other ground robots and vehicles.

Since no data training is included in current network, we also statistically investigated the success rate of collision detection under four candidate firing thresholds (Table 2). Each test of a specific threshold was held within a time window of approximately three-minutes. The results demonstrate that although this work is strict with parameter setting, it performed well in all situations – the success rates stayed close to the optimal one (95.3%).

<sup>1</sup>Two video demos of arena tests are in attached supplementary data.

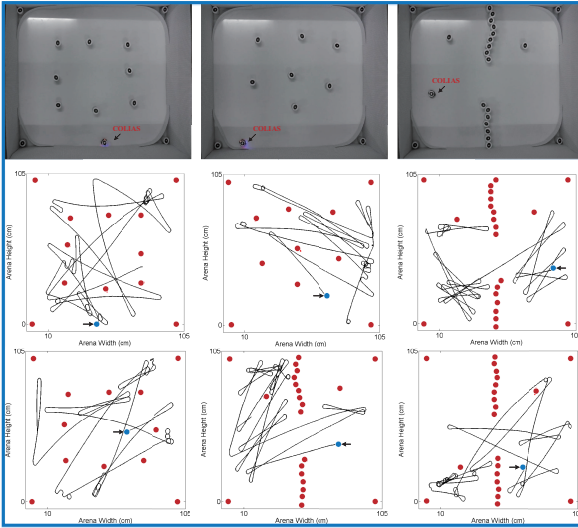


Figure 3: Top-down arena views and example results of Colias overtime-trajectories (dark lines). Red circles indicate obstacles varied in layouts. Blue ones denote the start position of Colias. There are four obstacles standing at corners of arena with regard to run a localization system [14].

### 4.3 Comparative Experiments

In order to clarify the advantages of this network, we did model comparison with a LGMD1 collision detector regarding to the modeling work in [56]. Both LGMDs vision systems were challenged by approach, recession and translation stimuli which constitute the general occasions in the daytime navigation of ground robots.

Firstly, when challenged against looming object, all collision-avoidance behaviors were shut down. We received the model outputs via the DCMI of robot connecting with the hosts. Colias was initiated to approach a same fixed dark object in the bright environment, at three constant speed levels – 5, 15 and 30 cm/s respectively, from an initial distance of 50cm (Fig. 4(a)). The results illustrate that both LGMDs neurons elicit vigorous potentials when closing in the target with varied time windows pertaining to different speeds. As the speed-level increased, the responses of both LGMDs climb up more significantly, especially the exponentially mapped membrane potential of LGMD2. On the other hand, at the beginning of receding from the object, LGMD1-Colias was read out ramping up potentials resembling an approach-level. Nevertheless, the sparse and low-level EMPs were witnessed from the readouts of LGMD2-Colias (Fig. 4(b)).

Moreover, we examined the relevance of speed and distance to collision-detecting (DTC). The statistical results in Fig. 5 represent that the collected DTC data of both vision systems rise along with speed increasing. Compared to LGMD1, the error-curve (information with variance and mean) of LGMD2 grows much more steeply which reveals a better speed response to potential collision in the case of LGMD2 framework. The proposed network was also challenged by varied-shaped objects in approaching-trials respectively. The DTC results demonstrate an invariance of LGMD2 framework to the shape of targets (Fig. 5).

At the final step, we inspected the model response against X-Y planes movements. The



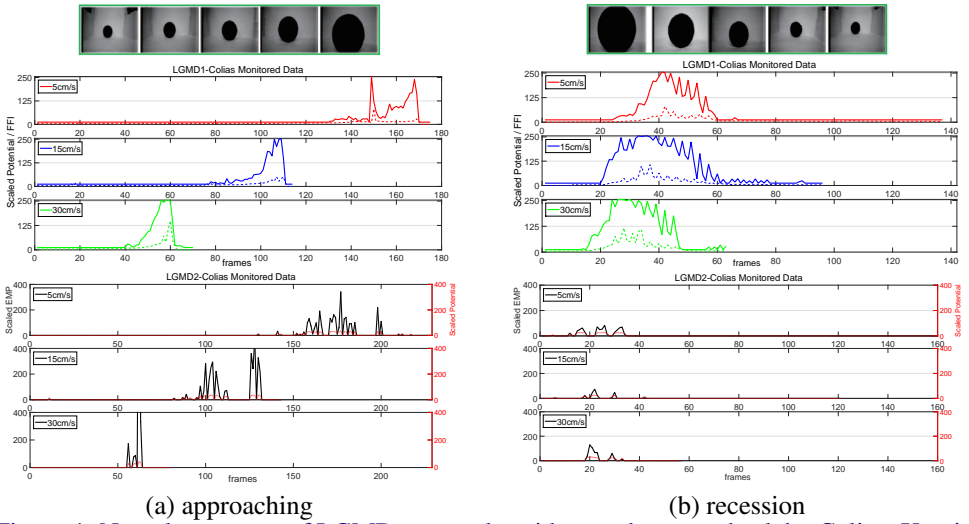


Figure 4: Neural responses of LGMDs networks with snapshots sent back by Colias. X-axis denotes the time course in frames and Y-axis indicates the scaled potential and FFI (dashed) for LGMD1, the scaled EMP and potential (dashed) for LGMD2 respectively.

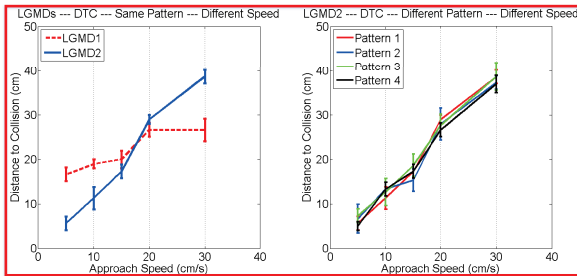


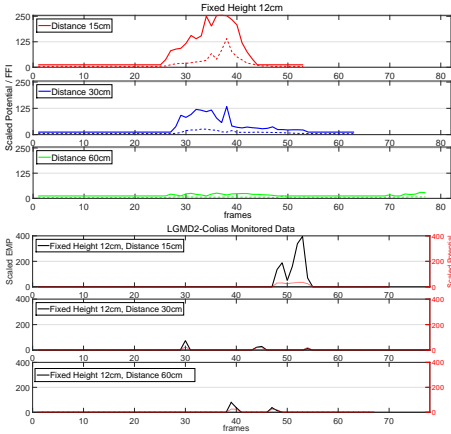
Figure 5: Statistic DTC error-curves. Both kinds of tests included 5 speeds, each of which repeated 3 times.

experimental setting is shown in Fig. 6(a) – we let the ball automatically roll down along a slot, forming the horizontal translating stimulus. The two LGMDs vision systems were alternately challenged. In the first situation, the gradient was fixed (12cm in height), leading to nearly the same translating speed. The observing distance varied in 15, 30 and 60cm. The results illustrate LGMD1 neuron elicits lower-level potentials along with the monitoring distance increasing (Fig. 6(b)). And it could also be quiet at the distance of 60cm which is far enough for the micro-robot. Whereas LGMD2 neuron keeps quiet in almost situations, except that object translating at the distance of 15cm which rigorously activating LGMD2 detector. In the second case, the monitoring distance was fixed at 30cm with gradually increasing gradients (8, 12, 16cm), corresponding faster translating speed. It is not surprise that the LGMD2 response are not brisker, while the LGMD1 detector depicted more steeply increasing potentials as the stimulus speeding up (Fig. 6(c)).

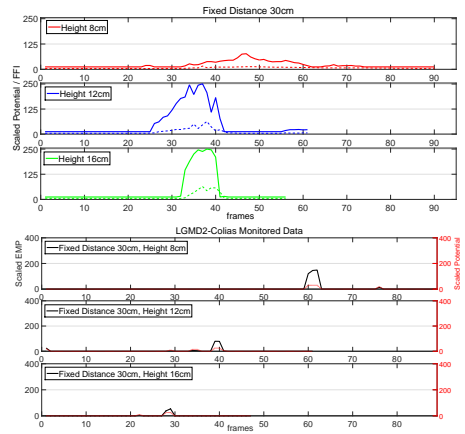
Through comparative investigations, the advantages of LGMD2 collision detector have been pinpointed: it represents better speed response to possible collision and convincible per-



(a) environment setting-up



(b) fixed gradient – varied distances



(c) fixed distance – varied gradients

Figure 6: LGMDs vision system challenged against systematic translation trials

formances coping with recession and translation of dark objects against bright environment in robotic vision system.

## 5 Conclusion

In this paper, we propose a bio-inspired collision detector based on the juvenile locust visual pathway. Compared to other computer vision techniques, this computational framework only involves low-level image processing methods, which performs quickly and robustly in a vision-based ground miniature robot. And in comparison with a related neural collision detector, we have two main contributions. First, the collision selectivity to dark objects against bright background is enhanced which makes it ideal for ground mobile robots. Second, the selectivity to approaching objects versus translation has been shaped which is expected for a practical collision-detecting system.

In the future work, we are interested in learning methods for network training. Our hope is this work will provide help toward our understanding of more complex functions of the visual nervous system and bring benefit to vision-based applications.

## Acknowledgments

This work was supported in part by EU FP7-IRSES Project EYE2E (269118) and LIVCODE (295151).

## References

- [1] M. D. Adams. *Sensor Modeling, Design and Data Processing for Autonomous Navigation*. River Edge, NJ: World Scientific, 1998.
- [2] Farshad Arvin and Masoud Bekravi. Encoderless position estimation and error correction techniques for miniature mobile robots. *Turkish Journal of Electrical Engineering and Computer Sciences*, 21(6):1631–1645, 2013.
- [3] Farshad Arvin, John Murray, Chun Zhang, and Shigang Yue. Colias: An autonomous micro robot for swarm robotic applications. *International Journal of Advanced Robotic Systems*, pages 1–10, 2014.
- [4] G. Benet, F. Blanes, J. E. Simo, and P. Perez. Using infrared sensors for distance measurement in mobile robots. *Robot. Autom. Syst.*, 40:255–266, 2002.
- [5] S. Bermudez i Badia, U. Bernardet, and P. F. Verschure. Non-linear neuronal responses as an emergent property of afferent networks: a case study of the locust lobula giant movement detector. *PLoS Comput Biol*, 6(3):e1000701, 2010. doi: 10.1371/journal.pcbi.1000701.
- [6] A. Borst and M. Egelhaaf. Principles of visual motion detection. *Trends Neurosci*, 12: 297–306, 1989.
- [7] A. Borst and T. Euler. Seeing things in motion: models, circuits, and mechanisms. *Neuron*, 71(6):974–94, 2011. doi: 10.1016/j.neuron.2011.08.031.
- [8] D. A. Clark, L. Bursztyn, M. A. Horowitz, M. J. Schnitzer, and T. R. Clandinin. Defining the computational structure of the motion detector in drosophila. *Neuron*, 70(6): 1165–1177, 2011. doi: 10.1016/j.neuron.2011.05.023.
- [9] G. N. DeSouza and A. C. Kak. Vision for mobile robot navigation: a survey. *IEEE Trans. Pattern Anal. Mach. Intell.*, 24(2):237–267, 2002.
- [10] H. Eichner, M. Joesch, B. Schnell, D. F. Reiff, and A. Borst. Internal structure of the fly elementary motion detector. *Neuron*, 70(6):1155–64, 2011. doi: 10.1016/j.neuron.2011.03.028.
- [11] H. R. Everett. *Sensors for Mobile Robots: Theory and Application*. Wellesley, MA: AK Peters, 1995.
- [12] Arvin F., Turgut AE., Tomas Krajnik, and Yue S. Investigation of cue-based aggregation in static and dynamic environments with a mobile robot swarm. *Adaptive Behavior*, 24(2):102–118, 2016.
- [13] Qinbing Fu and Shigang Yue. Modelling lgmd2 visual neuron system. In *2015 IEEE 25th International Workshop on Machine Learning for Signal Processing (MLSP)*, pages 1–6. IEEE.
- [14] F. Gabbiani and P. W. Jones. A genetic push to understand motion detection. *Neuron*, 70(6):1023–5, 2011. doi: 10.1016/j.neuron.2011.06.005.

- [15] F. Gabbiani, H. G. Krapp, N. Hatsopoulos, C. H. Mo, C. Koch, and G. Laurent. Multiplication and stimulus invariance in a looming-sensitive neuron. *J Physiol Paris*, 98(1-3):19–34, 2004. doi: 10.1016/j.jphysparis.2004.03.001.
- [16] Fabrizio Gabbiani, Gilles Laurent, Nicholas Hatsopoulos, and Holger G. Krapp. The many ways of building collision-sensitive neurons. *Trends in Neurosciences*, 22(10):437–438, 1999. ISSN 01662236. doi: 10.1016/s0166-2236(99)01478-2.
- [17] Meng H., Yue S., Hunter A., Appiah K., Hobden M., Priestley N., Hobden P., and Pettit C. A modified neural network model for lobula giant movement detector with additional depth movement feature. In *Neural Networks, IJCNN 2009 International Joint Conference.*, pages 2078–2083. IEEE.
- [18] Bin Hu, Shigang Yue, and Zhuhong Zhang. A rotational motion perception neural network base on asymmetric spatiotemporal visual information processing. *IEEE Transactions on Neural Networks and Learning Systems*, 2016.
- [19] Cheng Hu, Farshad Arvin, Caihua Xiong, and Shigang Yue. A bio-inspired embedded vision system for autonomous micro-robots: the lgmd case. *IEEE Transactions on Cognitive and Developmental Systems*, 2016.
- [20] G. Indiveri and R. Douglas. Neuromorphic vision sensors. *Science*, 288:1189–1190, 2000.
- [21] Tomas Krajník, Matias Nitsche, Jan Faigl, Petr Vanek, Martin Saska, Libor Preucil, Tom Duckett, and Marta Mejail. A practical multirobot localization system. *Journal of Intelligent and Robotic Systems*, 76(3-4):539–562, 2014. ISSN 0921-0296/1573-0409. doi: 10.1007/s10846-014-0041-x.
- [22] O’Shea M. and Williams J. L. D. The anatomy and output connections of a locust visual interneurone: the lobula giant movement detector (lgmd) neurone. *J Comp Physiol*, 91(257-266), 1974.
- [23] O’Shea M. and C. H. F. Rowell. The neuronal basis of a sensory analyser, the acridid movement detector system. ii. response decrement, convergence, and the nature of the excitatory afferents to the fan-like dendrites of the lgmd. *J Exp Biol*, 65:289–308, 1976.
- [24] R. Manduchi, A. Castano, A. Talukder, and L. Matthies. Obstacle detection and terrain classification for autonomous off-road navigation. *Autonomous Robots*, 18:81–102, 2005.
- [25] F. C. Rind and Bramwell D. I. Neural network based on the input organization of an identified neurone signaling impending collision. *J Neurophysiol*, 75:967–985, 1996.
- [26] F. C. Rind and P. J. Simmons. Seeing what is coming: Building collision sensitive neurons. *Trends Neurosci.*, 22:215–220, 1999.
- [27] A. Rosenfeld. From image analysis to computer vision: an annotated bibliography. *Comput. Vis. Image Understanding*, 84:298–324, 2001.
- [28] Yue Shigang and F.C. Rind. Near range path navigation using lgmd visual neural networks, Aug. 2009.

- [29] P. J. Simmons and F. C. Rind. Responses to object approach by a wide field visual neurone, the lgmd2 of the locust: Characterization and image cues. *J Comp Physiol A*, 180:203–214, 1997.
- [30] R. Stafford, R. D. Santer, and F. C. Rind. A bio-inspired visual collision detection mechanism for cars: combining insect inspired neurons to create a robust system. *Biosystems*, 87(2-3):164–71, 2007. doi: 10.1016/j.biosystems.2006.09.010.
- [31] J. Sztarker and F. C. Rind. A look into the cockpit of the developing locust: looming detectors and predator avoidance. *Dev Neurobiol*, 74(11):1078–95, 2014.
- [32] S. Wernitznig, F. C. Rind, P. Polt, A. Zankel, E. Pritz, D. Kolb, E. Bock, and G. Leitinger. Synaptic connections of first-stage visual neurons in the locust *schistocerca gregaria* extend evolution of tetrad synapses back 200 million years. *J Comp Neurol*, 523(2):298–312, 2015. doi: 10.1002/cne.23682.
- [33] S. D. Wiederman, P. A. Shoemaker, and D. C. O’Carroll. Correlation between off and on channels underlies dark target selectivity in an insect visual system. *J Neurosci*, 33(32):13225–32, 2013. doi: 10.1523/JNEUROSCI.1277-13.2013.
- [34] S. Yue and F.C.Rind. Visually stimulated motor control for a robot with a pair of lgmd visual neural networks. *Int. J. Adv. Mechatron. Syst.*, 4(5):237–247, 2012.
- [35] S. Yue and F. C. Rind. A collision detection system for a mobile robot inspired by locust visual system. In *Proc. IEEE Int. Conf. Robot. Autom.*, pages 3843–3848, 2005.
- [36] S. Yue and F. C. Rind. Collision detection in complex dynamic scenes using a lgmd based visual neural network with feature enhancement. *IEEE Trans. Neural Netw.*, 17(3):705–716, 2006.
- [37] S. Yue and F. C. Rind. Near range path navigation using lgmd visual neural networks, Aug. 2009.
- [38] Shigang Yue and F. Claire Rind. Visual motion pattern extraction and fusion for collision detection in complex dynamic scenes. *Computer Vision and Image Understanding*, 104(1):48–60, 2006.
- [39] Shigang Yue, F. Claire Rind, Matthais S. Keil, Jorge Cuadri, and Richard Stafford. A bio-inspired visual collision detection mechanism for cars: Optimisation of a model of a locust neuron to a novel environment. *Neurocomputing*, 69(13-15):1591–1598, 2006.
- [40] Shigang Yue, Roger D. Santer, Yoshifumi Yamawaki, and F. Claire Rind. Reactive direction control for a mobile robot: a locust-like control of escape direction emerges when a bilateral pair of model locust visual neurons are integrated. *Autonomous Robots*, 28(2):151–167, 2010.